J Appl Electrochem (2008) 38:869–874
DOI 10.1007/s10800-008-9531-5

ORIGINAL PAPER

Effect of carbon surface oxidation on platinum supported carbon particles on the performance of gas diffusion electrodes for the oxygen reduction reaction

Ahmad Nozad Golikand · Elaheh Lohrasbi · Mohammad Ghannadi Maragheh · Mehdi Asgari

Received: 19 November 2007 / Revised: 19 February 2008 / Accepted: 21 February 2008 / Published online: 14 March 2008

Abstract The effect of carbon surface oxidation on platinum supported carbon particles (Pt/C) with nitric acid was investigated by cyclic voltammetry, electrochemical impedance spectroscopy, polarization experiments and chronoamperometry. Cyclic voltammograms, polarization curves and electrochemical impedance spectra showed that the treated catalyst had much larger active surface area and higher ionic conductivity than the untreated catalyst, and provided enhanced performance for oxygen reduction. The formation of acidic groups was examined by IR spectra. The Pt/C surface oxidation had a large effect on the performance of a gas diffusion electrode for oxygen reduction reaction.

Keywords Surface oxidation · Carbon supported catalyst · Gas diffusion electrode · Catalyst layer · Oxygen reduction reaction

1 Introduction

The cathode catalyst layer of polymer electrolyte membrane fuel cells (PEMFCs) consists of a proton conducting ionomer, carbon particles and Platinum particles. Increasing the Nafion content in the catalyst layer improves proton migration, however, it reduces void space, thus worsening gaseous oxygen transport. Increasing the Pt loading enhances the rate of the electrochemical reaction but increases the cost.

A. N. Golikand (✉) · M. G. Maragheh · M. Asgari
Jaber Ibne Hayan Research Labs., Chemistry Department, NSTRI, Tehran, Iran
e-mail: ahmadnozadgolikand@yahoo.com

A. N. Golikand · E. Lohrasbi
Corrosion Lab., Material School, NSTRI, Tehran, Iran

Achieving a compromise between Nafion content and Pt loading poses a challenge for the improvement of the catalyst layer performance because it involves complex transport and electrochemical reaction phenomena that take place in the composite and porous media [1]. Accordingly there is a limit on the quantity of Nafion that needs to be added without any effect on the cell performance. In recent years, certain new approaches such as introduction of proton-conducting agents in the catalyst carbon support have been adopted to improve the performance of PEM fuel cells [2–5].

Recently, Selvarani et al. [6] anchored phenyl-sulphonic group on the carbon support of the Platinum catalyst, and Jiang et al. [7] modified the surface of carbon nanotubes by the addition of hydrogen peroxide during the chemical vapor deposition synthesis. In their study, FTIR experiments showed that there were C–OH and C–O–C functional groups on the carbon nanotube (CNT) walls. Also, Guo and Rockstraw [8] prepared activated carbon from rice hull by one step phosphoric acid activation, and demonstrated that carbon products with relative low ash content and high activation degree could be prepared from rice hull by H_3PO_4 activation at suitable temperature.

Natarajan and Hamelin [9] studied the chemical oxidation of carbon nanotubes with 1:1 proportion of 7.5 M H_2SO_4 and 15 M HNO_3 solutions.

Kim et al. [10] reported that microwave nitrogen plasma treatment can considerably change the surface chemistry of carbon black and bring surface nitrogen functionality such as –NH, C–N, =NH, – NH_3^+, C=N, and NH_2 groups, leading to improvement of the deposited capacity of Pt catalyst. Oda et al. [11] prepared activated carbon fibers with various amount of functional groups by a redox method. Park and Kim [12] reported that electrochemical treatment of carbon black in an aqueous potassium

hydroxide solution, as a function of the electric current, led to a modification of carbon surface properties, i.e., pH, acid–base values, anion exchange and microstructure.

Li et al. [13] proposed that the morphology, crystallinity and surface properties of carbon nanotubes can be modified by pretreatment with oxidative mineral acids (HNO_3, mixed $HNO_3 + H_2SO_4$ and $K_2Cr_2O_7 + H_2SO_4$). They showed that the deposition of 20% Pt on the pretreated carbon nanotube supports by a modified colloidal method led to Pt/CNT catalyst with the average Pt particle size of approximately 3.0 nm.

Antonucci et al. [14] studied the interaction between platinum crystallites and surface functional groups of Pt/C catalyst for phosphoric acid fuel cells.

In the present work, the effect of carbon surface oxidation on Pt/C with nitric acid was investigated by cyclic voltammetry, electrochemical impedance spectroscopy, polarization experiments and chronoamperometry.

2 Experimental

2.1 Anchoring acidic groups to carbon-supported platinum catalyst

A commercial catalyst (20% Pt on XC- 72R from Electro Chem Inc) was heated under reflux in concentrated nitric acid for 40 min. It was then washed well with deionized water and dried to produce a treated catalyst.

2.2 Fabrication of gas diffusion electrode and electro chemical measurements

Porous GDE was constructed according to a previously described procedure [15]. To prepare the PTFE- bonded porous GDL, a commercially available carbon Vulcan (XC- 72R from ElectroChem Inc) 70% and 30% PTFE (from ElectroChem Inc) emulsion were used and painted on to carbon paper TGP-H-0120 (Toray). The resulting composite structure was dried in air at 80–90 °C for 1 h, followed by thermal treatment at 250 °C for 30 min to remove the dispersion agent contained in the PTFE, and finally sintered in air at 340 °C for 15 min. The PTFE is effective as a binder and imparts hydrophobicity to the gas diffusion regime of the electrode.

To prepare the catalyst layer, a mixture comprising a homogeneous suspension of Nafion, Pt/C catalyst and Isopropyl alcohol as solvent was homogenized using a sonicator (Misonix Model S-3000) for 20 min. The ink was painted on the GDL. The resulting composite structure was dried in air at 25 °C for 1 h and finally sintered in air at 140 °C for 45 min.

Nafion and Pt loadings were 1 mg cm^{-2} and 0.5 mg cm^{-2} in the GDE, respectively, when the untreated Pt/C was used in the catalyst layer, while the Nafion loading changed in the range 0.5–1 mg cm^{-2} and Pt loading changed in the range 0.2–0.5 mg cm^{-2} when the treated Pt/C was used in the catalyst layer (Table 1).

The reduction of oxygen was investigated with the porous GDE (geometric exposed area of 1.3 cm^2) in 2 M H_2SO_4 solution. Linear sweep voltammetry (LSV) measurements were carried out at 298 K, in a conventional three-electrode cell, with O_2 flow rate of 50 ml min^{-1}. The cyclic voltammetry (CV) experiments were done under Argon atmosphere. The GDEs were mounted in a Teflon holder containing a high pyrolytic graphite disk as a current collector (which had arrangement for oxygen feed from the back of the electrode). A large-area platinum flat electrode was used as the counter electrode. An Ag/AgCl reference electrode was placed close to the working electrode surface. The electrochemical cell was connected to a potentiostat-galvanostat (Radiometer Model DEA332) digital electrochemical analyzer equipped with an IMT 102 electrochemical interface, for the CV, chronoamperometry and LSV, and also to a computer controlled 302 Autolab electrochemical system (EcoChemie, Utrecht, Netherland), driven with GPES and FRA software (EcoChemie) for electrochemical impedance spectroscopy (EIS). In the present work, an AC potential amplitude of 5 mV in a frequency range 1 mHz to 10 kHz was applied.

Table 1 The charges, Q_H and EAS for the tested electrodes extracted from the voltammograms of Figs. 1 and 2

Number of electrode	Loadings	Q_H (mC)	A_r (cm^2)	EAS (m^2 g^{-1})
GDE1	Unmodified, LNa = 1, Lpt = 0.5	253	1204.7	240.9
GDE2	Modified, LNa = 1, Lpt = 0.5	538	2561.9	512.3
GDE3	Modified, LNa = 0.8, Lpt = 0.5	818	3895.2	779.1
GDE4	Modified, LNa = 0.7, Lpt = 0.5	352	1676.1	335.2
GDE5	Modified, LNa = 0.5, Lpt = 0.5	234	1114.2	222.8
GDE6	Modified, LNa = 1, Lpt = 0.4	766	3647.6	729.5
GDE7	Modified, LNa = 1, Lpt = 0.3	440	2095.2	419.04
GDE8	Modified, LNa = 1, Lpt = 0.2	133	633.3	126.6

Infrared spectra in the region of 400–4000 cm^{-1} were recorded in KBr pellets using a BRUCKER vector 22 FT-IR spectrophotometer. The spectrum obtained after multiple scans is a plot of transmittance percent against wave number.

3 Results and discussion

3.1 Cyclic voltammetry study

Cyclic voltammetry was carried out to understand the variation of electrochemical surface area (ESA) with modification of Pt/C with Nafion and Pt loadings in the catalyst layer.

The voltammograms of electrodes, with constant Pt loading of 0.5 mg cm^{-2} and different Nafion loading, with modified Pt/C and unmodified Pt/C in the catalyst layer, are presented in Fig. 1. From a physical point of view, Nafion loading mostly influences the ionic resistance of the catalytic layer. At 0.8 mg cm^{-2} Nafion (GDE3), a maximum electrochemical activity was found, and correspondingly, the ionic resistance of the electrode reached its lowest value (as listed in Table 2). This phenomenon has been explained according to a physical model based on the fact that, for a low amount of Nafion, the electrolyte is located within the pores of the electrodes, and resistance decrease when the pores fill with Nafion. Above 0.8 mg cm^{-2} (e.g. GDE2) Nafion, due to the hydrophobic–hydrophilic properties of the Nafion structure, a further supply of electrolyte does not fill the pores but forms films on the external surface of the electrodes, giving an additional contribution to the overall resistance. Moreover, excess Nafion added in the catalyst layer lowers the performance of PEMFCs, because the diffusion of the reactant gases to Pt catalyst sites is disturbed. The excess addition leads to the reduction of reaction currents due to lowering of the diffusion rate of the reactant gases in the Nafion film covering Pt catalyst particles. Although, in the present work the performance was reduced by excess addition of Nafion, an increase in electrochemically active surface area was observed with increasing of Nafion loading (as shown in Table 1), since the ionic conductivity of the catalyst layer increased due to non-operating measurement of the active surface area. It seems that this was not straight related to the resistance and gas diffusion limitation. Nafion was impregnated in to the modified catalyst to investigate its effect on the ORR performance. The results indicated that 1 mg cm^{-2} of Nafion in the modified catalyst layer (e.g. GDE2) decreased its performance. This observation is contrary to the fact that impregnation of Nafion into commercial carbon-supported catalyst usually improves the catalyst performance in ORR [16], probably because the modified catalyst provides sufficient ionic conductivity. Further addition of Nafion to the catalyst layer would block O_2 diffusion to the Pt surface and give a lower ORR performance. This advantage for modified catalyst will further reduce costs of PEMFCs, since Nafion is one of their most expensive components. Also, Fig. 1 displays CVs for the modified and original catalyst, indicating that the HNO_3 treated catalyst behaved somewhat differently from the original catalyst. As Fig. 1 shows, the treated catalyst had larger hydrogen adsorption and desorption peaks corresponding to a higher active catalyst surface area. Charge integration of hydrogen adsorption for the treated and non-treated catalyst, gave active surface areas of 779.04 $m^2\ g^{-1}$ and 240.95 $m^2\ g^{-1}$, respectively. The active surface area can be calculated as descripted latter. Furthermore, there was a new (or enlarged) redox peak, most likely corresponding to a quinone-hydro quinine couple [17] associated with the treated catalyst. It can be concluded that the oxidation of the carbon support significantly increases the acidic functional groups such as –OH and –COOH, so that proton eccess to the catalyst surface is much easier, leading to a larger active surface area. This is one of the main reasons that the modified catalyst improves

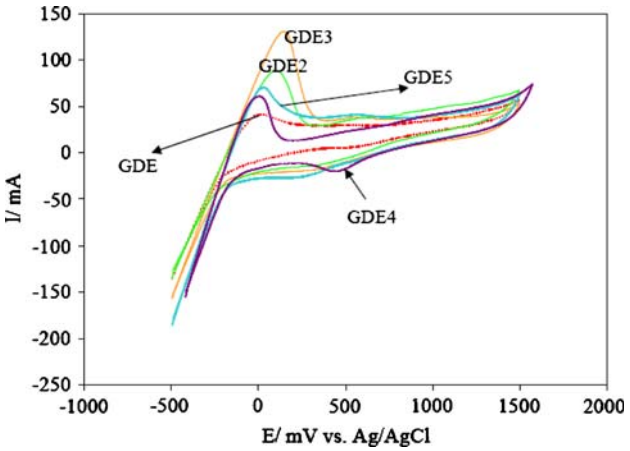

Fig. 1 The voltammograms of electrodes, each with a Pt loading of 0.5 mg cm^{-2} and with a different Nafion loading in the catalyst layer (Scan rate; 50 mV s^{-1}, temperature; 25 °C)

Table 2 The ionic resistance of the tested electrodes, extracted from Fig. 4

Number of electrode	R_{ionic} (Ω)
GDE1	2.4
GDE2	0.9
GDE3	0.3
GDE4	0.4
GDE5	0.9
GDE6	1.0
GDE7	4.2
GDE8	3.8

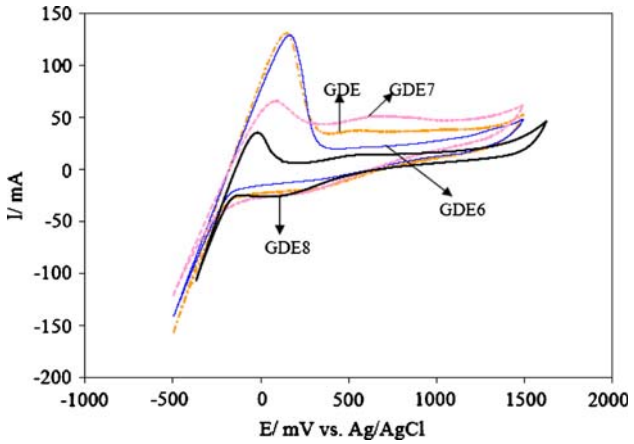

Fig. 2 The voltammograms of electrodes, each with a Nafion loading of 1 mg cm^{-2} and with a different Pt loading in the catalyst layer (Scan rate; 50 mV s^{-1}, temperature; 25 °C)

ORR performance. The chemical oxidation also causes profound modification of the morphological characteristics of the carbon support (i.e., increase in micro porosity) [18] and significantly increases its wettability because of the increased acidic functional groups. The increase in wettability is attributed to an increased pore volume and to the progressive build-up of oxygenated groups.

The voltammograms of electrodes, with a constant Nafion loading of 1 mg cm^{-2} but a different Pt loading (with modified Pt/C and unmodified Pt/C in the catalyst layer) are presented in Fig. 2.

To determine the EAS, the charge due to adsorbed hydrogen (Q_H) was obtained by integration of the corresponding peak in the voltammogram with a double layer charging current as a base line. Table 1 summarizes the charges Q_H and EAS for the tested electrodes. Table 1 shows EAS calculated at different Nafion loadings and different Pt loadings in the catalyst layer by means of Eq. 1 [19].

$$\mathrm{EAS} = \frac{Q_H}{[\mathrm{Pt}] \times 0.21} \tag{1}$$

where, [Pt] represents the Platinum loading (mg cm^{-2}) in the electrode, Q_H is the charge for hydrogen desorption (mC cm^{-2}) and 0.210 represents the charge required to oxidize a monolayer of H_2 on bright Pt [20–22].

Table 1 summarizes the charges Q_H and EAS for the tested electrodes shows increasing EAS with modification of Pt/C in the catalyst layer. However the results indicate the same EAS for the modified Pt/C with the Nafion loading of 0.5 mg cm^{-2} (e.g.GDE5) and for the unmodified Pt/C with Nafion loading of 1 mg cm^{-2} (e.g.GDE1).

Ideally, it would be preferable to use modified Pt/C to decrease the amount of proton exchange polymer needed in the catalyst layer for optimum performances.

Table 1 shows increased EAS for the GDE7 comparing to the GDE1. It shows that the Pt loading used in GDEs can be reduced with modification of the Pt/C. An increase in Platinum utilization was found after anchoring the acidic group to the carbon support, due to extension of three-phase boundary in the catalyst layer, especially inside the carbon agglomerate through the acidic group [17]. This finding is further illustrated by the modified schematic diagram of the internal structure for the catalyst layer by Uchida et al. [23] (Fig. 3).

3.2 Determination of kinetic parameters

In order to obtain kinetic parameters for the oxygen reduction reaction at fabricated GDEs, a Tafel plot was used. The data were fitted by equation [24].

$$E = E_0 - b\,\log(i) - iR \tag{2}$$

where

$$E_0 = E_r + b\log\,(i_0) \tag{3}$$

In Eqs. 2 and 3, i_0 is the exchange current density for oxygen reduction, b the Tafel slope, E_0 the reversible potential for the oxygen electrode reaction and R represent the resistance (predominantly the ohmic resistance of the electrolyte) responsible for the linear variation of potential with current density. Equation 2 is valid to the end of the linear region of the potential versus current density plot. At high current density, the difference in the E versus i data from Eq. 2 is due to the rapidly increasing contribution of mass-transport over potentials. The parameters E_0, b and R were evaluated by a nonlinear least squares fitting of Eq. 2 to the experimental data. Using the R values, the iR-corrected Tafel plots ($E + iR$ versus log i) were obtained. Variations of exchange current density with the modified and unmodified Pt/C in GDEs are shown in Table 3.

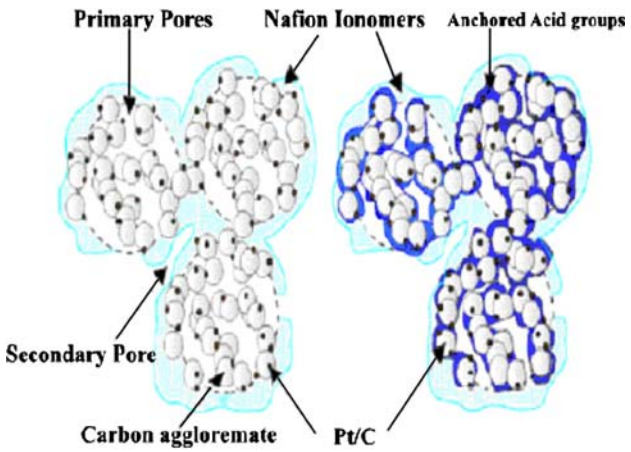

Fig. 3 Schematic illustration of electronic and ionic conduction paths in the catalyst layer for the unmodified and modified catalyst

Table 3 Variation of exchange current density with the modified and unmodified Pt/C that have used in preparation of GDEs

Number of electrode	Exchange current (mA cm^{-2})
GDE1	4.2
GDE2	12.2
GDE3	2.8
GDE4	7.2
GDE5	2.7
GDE6	2.4
GDE7	5.9
GDE8	0.8

The exchange current density is highest for GDE2. Thus the treatment of Pt/C in GDEs, provided conditions, that led to an optimum structure in the reaction layer. At zero exchange current density no reaction can occur. This exchange current density is crucial to the control of the performance of GDEs. Increasing the value of the exchange current density reduces the voltage drop [25].

3.3 Chronoamperometry

Chronoamperometry was used to quantitatively compare the diffusivity of oxygen in GDEs, according to [7]:

$$i(t) = nFA(D/\pi t)^{1/2}C^* \quad (4)$$

where, i is the current (mA); n is the number of electrons; F is the Faraday constant (96485 C mol^{-1}); A is the surface area of the electrode (cm^2); D is the diffusion coefficient (cm^2 s^{-1}); t is the time (s) and C^* is the concentration of the reactant (mM).

One can define $D^{1/2}C^*$ as permittivity of oxygen at the GDE. A Cottrell plot can be obtained from chronoamperometry (i vs. $t^{-1/2}$). The permittivity can be calculated from the slope of this curve. The permittivity values of the GDEs are given in Table 4. The value of permittivity for GDE 3 is more than that of the other GDEs.

Table 4 The diffusion coefficient of the tested electrodes, extracted from the chronoamperometry data

Number of electrode	$\left(C^*D^{0.5}/\mathrm{cm}^{-2}s^{-0.5}\right) \times 10^{-6}$
GDE1	0.93
GDE2	1.11
GDE3	1.76
GDE4	1.47
GDE5	0.89
GDE6	0.87
GDE7	0.16
GDE8	0.15

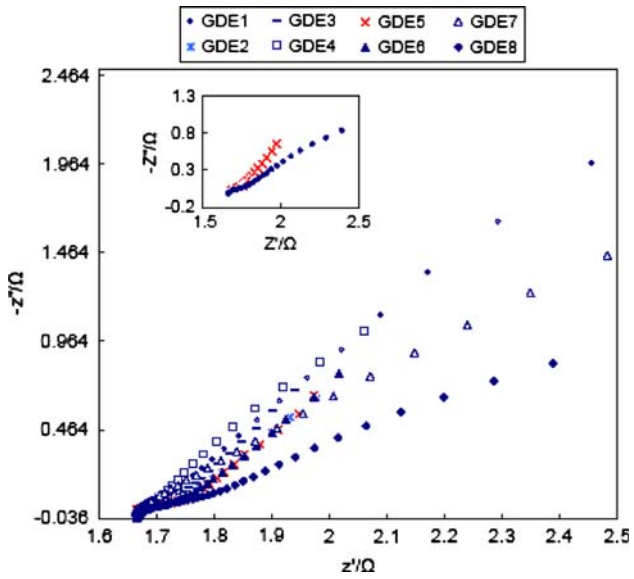

Fig. 4 Impedance data in the Nyquist representation obtained at open circuit voltage under argon reflux in 298 K

3.4 Electrochemical impedance spectroscopy

Electrochemical impedance spectroscopy was used to characterize the ionic resistance, where impedance spectra were recorded at the open circuit voltage and under Argon reflux. We also assume that diffusion and kinetic impedances associated with faradaic process are negligible because the electrodes were purged with argon prior to, and during, the impedance measurements. At high frequencies a Warburg-like response is observed, corresponding to ion migration through the catalyst layer. The ionic resistance, R_{ionic}, can be obtained from the length of the Warburg-like region projected on to the real impedance (Z') axis ($=R_{\text{ionic}}/3$) [26]. Figure 4 shows the impedance spectra in the form of a Nyquist plot. Data from these diagrams are shown in Table 2. These show that in GDE 2, the ionic resistance is lower than in GDE 1, confirming the previous outcomes about GDE2.

3.5 IR spectra of modified catalyst

Figure 5 shows IR spectra for the carbon-supported catalyst treated by HNO_3 and unmodified Pt/C. Almost no acidic functional groups were detected on the original catalyst surface. The HNO_3 treated catalyst showed an absorption peak at 1280 cm^{-1}, may be due to a mixture of carboxylic and carbonyl groups [27]. An absorption peak is also found at around 3400 cm^{-1} related to an OH stretch, probably due to water adsorption. In either case, this indicates that the modified catalyst becomes more hydrophilic. Oxidation of carbon support in HNO_3 causes a large increase in the concentration of the surface oxide groups.

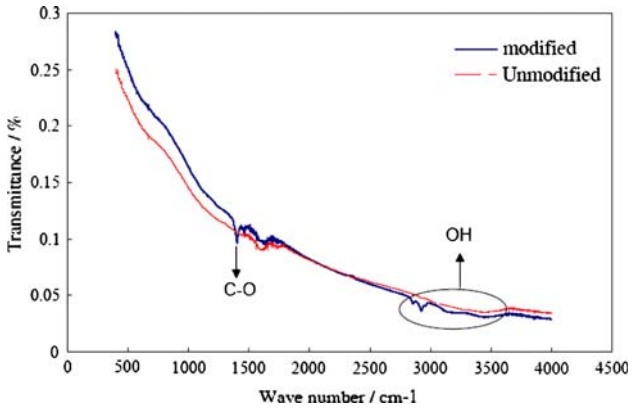

Fig. 5 IR spectra of the modified and unmodified Pt/C in KBr disk

This fact has been confirmed by CVs for the treated catalyst which showed an additional oxidation peak associated with –OH (Fig. 1).

Furthermore, the pH of an aqueous slurry of carbon can also provide a convenient indicator of the surface groups. The pH of carbon slurries is thought to be a function mainly of the concentration of carboxylic acid groups. The complete titration of carbon slurries provides additional information on the surface properties. Accordingly, titration of a HNO_3-modified catalyst showed that it possessed an acidity twice as high as the non-treated catalyst (Martin and Pickup 1998 Personal Communication). Therefore, it can be concluded that the modified catalyst improves ORR performance due to its increased proton accessibility to the catalyst surface and also increased proton concentration. The increased concentrations of –OH and –COOH on the carbon surface also increase the ionic conductivity of the catalyst layer. This creates a potential advantage for the systems using Nafion as a binder and ionic conductor in their catalyst layer, since less amount of Nafion will be required. This would decrease O_2 diffusion limitations.

4 Conclusion

Electrodes prepared by carbon surface oxidation on Pt/C showed superior performance. It is suggested that anchoring the acidic group on the Pt/C enhances the performance of gas diffusion electrodes. This is achieved by increasing the utilization of Pt by enhancing the three-phase boundary in the catalyst layer. The electrode prepared with modified Pt/C and with Nafion and Pt loadings of 0.8 mg cm^{-2} and 0.5 mg cm^{-2} (e.g. GDE3), respectively, showed the best performance.

Moreover, a more hydrophilic carbon support will tend to associate with the sulfonic acid groups of the Nafion leaving the hydrophobic perfluorinated backbone to face the oxidant gas. This orientation will lead to a higher oxygen concentration in the catalyst layer (O_2 has a much higher solubility in non polar backbone) and should produce a much improved ORR performance.

As shown in Table 3, the exchange current density values are considerably greater for GDEs with modified Pt/C, which indicates easier oxygen reduction due to the formation of oxygenated groups.

Chronoamperograms were used to quantitatively compare the diffusivity of oxygen in GDEs. These results are consistent with the ability of oxygenated groups to enhance the diffusion of oxygen in the catalyst layer.

References

1. Song D, Wang Q, Liu Z et al (2005) Electrochim. Acta 50:3347
2. Yu Y, Kosbach L Modified carbon products useful in gas diffusion electrodes, US Patent 6,399,202
3. Xu Z, Qi Z, Kaufman A (2003) Electerochem Solid-State Lett. 6:A171
4. Srinivas B, Dotson AO Proton conductive carbon material for fuel cell applications. US Patent 2004/0109816 A1
5. Peng F, Zhang L, Wang H et al (2005) Carbon 43:2397
6. Selvarani G, Saha AK, Choudhury NA et al (2007) Electrochim Acta 52:4871
7. Jiang H, Zhu L, Moon KS et al (2007) Carbon 45:655
8. Guo Y, Rockstraw DA (2007) Microporous Mesoporous Mater 100:12
9. Natarajan SK, Hamelin J (2007) Electrochim Acta 52:3751
10. Kim S, Cho MH, Lee JR et al (2006) J Power Sources 159:46
11. Oda H, Yamashita A, Minoura S et al (2006) J Power Sources 158:1510
12. Park SJ, Kim JS (2001) Carbon 39:2011
13. Li L, Wu G, Xu BQ (2006) Carbon 44:2973
14. Antonucci PL, Alderucci V, Giordano N et al (1994) J Appl Electrochem 24:58
15. Uchida M, Aoyama Y, Eda N, Ohta A (1995) J Electrochem Soc 142:463
16. Poltarzewski Z, Statiai P, Alderucci V et al (1992) J Electrochem Soc 139:761
17. Wilson MS, Gotesfeld S (1992) J Appl Electrochem 22:1
18. Matsumura Y, Hagiwara S, Takahasha H (1976) Carbon 14:163
19. Pozio A, Francesco MD, Cemmi A et al (2002) J Power Sources 105:13
20. Perez J, Gonzalez ER, Ticianelli EA (1998) Electrochim Acta 44:1329
21. Ciureanu M, Wang H (1999) J Electrochem Soc 146:4031
22. Antolini E, Giorgi L, Pozio A, Passalacqua E (1999) J Power Sources 77:136
23. Uchida M, Fukuoka Y, Sugawara Y et al (1996) J Electrochem Soc 143:2245
24. Sirinivasan S, Ticianelli EA, Derouin CR, Redondo A (1988) J Power Sources 22:359
25. Larminie J, Dicks A (2000) Fuel cell systems explained. Wiley, New york
26. Lefebvre MC, Martin RB, Pickup PG (1999) Electrochem Solid-State Lett 2:259
27. O'reilly JM, Mosher RA (1983) Carbon 21:47